Preprints.org

Article

Synthesis, Characterization and Analytical Prospects of Cellulose-Derived Nanoparticles of Ferric-Oxide (Fe$_2$O$_3$/Cellulose) and Copper-Oxide (CuOx)

Sana Ullah Khan , Ali Khan , Amir Hassan [*]

Article

Synthesis, Characterization and Analytical Prospects of Cellulose-Derived Nanoparticles of Ferric-Oxide (Fe₂O₃/Cellulose) and Copper-Oxide (CuOx)

Sana Ullah Khan [1], Ali Khan [2] and Amir Hassan [3,*]

[1] Department of Chemistry, Government Post Graduate College, 23200 Mardan, Pakistan
[2] Department of Chemical and Materials Engineering, Chang Gung University, 333 Taiwan
[3] Faculty of Natural Sciences, Novosibirsk State University (NSU), 630090 Novosibirsk, Russia
* Correspondence: amirhassan741@gmail.com, a.khassan1@g.nsu.ru

Abstract: Our environment has been significantly impacted by man-made pollutants, primarily due to industries make substantial use of synthetic chemicals, resulting in significant environmental consequences. In this research investigation, the co-precipitation approach was employed for the synthesis of cellulose-based ferric oxide (Fe₂O₃/cellulose) and copper oxide nanoparticles (CuOx-NPs). Scanning electron microscopy (SEM) analyses were conducted to determine the properties of the newly synthesised nanoparticles. Furthermore, the synthesized nanoparticles were employed for eliminating chromium from aqueous media under various conditions, including temperature, contact time, adsorbent concentration, adsorbate concentration, and pH. Additionally, the synthesised materials were used to recover Cr(VI) ions from real samples, including tap water, seawater, and industrial water, and the adsorptive capacity of both materials evaluated under optimal conditions. The synthesis of Fe₂O₃/cellulose and CuOx-NPs proved to be effective, as indicated by the outcomes of the study.

Keywords: nanocomposites; cellulose-derived NPs; (Fe₂O₃/cellulose); (CuOx-NPs) and SEM

1. Introduction

Heavy metal ions which are transported into aquatic environment via industrial effluents affect aquatic life. They are harmful because of their hazardous bio-accumulative nature. One of the most hazardous heavy metal contaminants is Chromium Cr(VI), which has been utilized extensively and on a massive scale in a number of sectors, including metal cleaning, dyes, leather, textiles, and plating. Cr(VI) is a transition metal, steel-gray, lustrous, stiff, and having brittle appearance [1-4]. Cr(VI) has a high degree of oxidation resistance even at high temperatures. Cr(VI)   is exceedingly poisonous and carcinogenic; therefore its excess presence in food, water, or the environment may seriously harm the biota. For this reason, several environmental protection agencies have established a chromium limit that is acceptable as long as no acute or long-term effects on human health have been documented. According to the World Health Organization (WHO 1958), 0.05 mg/L of chromium is the maximum level that should be present in water. The Maximum Contaminant Limit (MCL) and Maximum Contaminant Limit Goal (MCLG) for chromium in water were both set at 0.1 parts per million (ppm) by the United States Environmental and Protection Agency (US EPA) in 2012. (100ppb). The Maximum Contaminant Limit (MCL) for chromium in drinking water is 0.05 mg/L, according to a 2013 report from the California Department of Public Health. The public health objective for Cr (VI) is 0.02 ppb; however the maximum contamination level is established at 10ppb. [4-5]. The quick removal of Cr (VI) ions from contaminated water has been focused from the last few decades and numerous techniques has been utilized such as electrochemical deposition, ion exchange, adsorption, biological methods, and membrane separation. Adsorption separation is the fastest, most practical, and least expensive method for the quick removal of harmful pollutants. The adsorptive removal of Cr(VI) ions from wastewater has occasionally been accomplished using a variety of adsorbents,

including zeolite, activated carbon, metal oxides, waste industrial material, and nano-composites, etc. For the quick removal of heavy Cr(VI) ions a variety of metal oxide nanostructures have been employed including cellulose based iron oxide nanoparticle composites, titanium oxides, aluminum oxides, and copper oxides [6-7].

In the present research investigations, synthesised Fe_2O_3/Cellulose nano-composites and CuOx-NPs are being characterised and used for the direct removal of Cr(VI) ions from an aqueous environment. Additionally, the adsorption properties of these adsorbents are being compared. The results obtained suggest that the synthesised Fe_2O_3/cellulose and CuOx-NPs are useful for adsorption and can potentially be used multiple times without losing their effectiveness.

2. Materials and Methods

2.1. Materials

The used papers served as a source of cellulose and were purchased from the local market. All of the reagents utilised in the experiment were of analytical grade. Iron(III) oxide, sodium hydroxide, copper chloride, copper nitrates, and urea were acquired from the commercial supplier Sigma-Aldrich.

2.2. Synthesis of Fe_2O_3/Cellulose Nanocomposite

Synthesis of Fe_2O_3/cellulose using the precipitation method involves a two-stage process. During the initial phase, previously utilised copy paper was fragmented into smaller segments, subjected to three rounds of washing with distilled water, and afterwards immersed in a solution containing 40% H_2SO_4. The mixture was subjected to filtration and afterwards washed four times with distilled water. Following this, the mixture was dried in an oven maintained at a temperature of 50 °C. In addition, a quantity of 3.3 gram of dried material was introduced into a solution containing NaOH, thiourea, and urea at a temperature of 261.15 Kelvin. The solution was then stirred for duration of 25 minutes in an environment saturated with nitrogen [8]. During the second stage of the experiment, a solution containing 15 ml of $Fe_2Cl_3.6H_2O$ (weighing 13.51g) and $FeCl_2.4H_2O$ (weighing 4.97g) was prepared. This solution was then added drop by drop to the cellulose solution and vigorously stirred for duration of 180 minutes at room temperature. The composite material that was synthesised underwent a filtration process, followed by rinsing with distilled water, ethanol, and acetone. The synthesised substance were further dried in an oven at a temperature of 323.15 K and thereafter stored.

2.3. Synthesis of CuOx-NPs

Copper oxide nanoparticles (CuOx-NPs) were synthesised utilising the precipitation method, employing copper chloride ($CuCl_2$) and copper nitrate ($Cu(NO_3)_2.3H_2O$) as precursor materials. To initiate the experiment, every precursor was initially dissolved in 100 millilitres of distilled water to achieve a concentration of 0.1 M. Subsequently, a 0.1 M NaOH solution was gradually introduced into the mixture under constant stirring until the pH level reached 14, resulting in the formation of black precipitates indicative of the presence of N_2 gas. The black precipitate was collected and later subjected to washing procedures until the pH was adjusted to 7.0. Distilled water was used initially, followed by a wash with 100% ethanol. The yields were thereafter subjected to a drying process at a temperature of 80 °C for duration of 16 hours, as indicated in references [9-10]. Subsequently, the synthesised materials passed through a calcination process at a temperature of 500 °C for duration of 4 hours.

2.4. Characterization and Batch Adsorption Study

The synthesised materials, which are Fe_2O_3/Cellulose and CuOx-NPs, were subjected to comprehensive characterization using essential analytical techniques. In order to determine the characteristics of the freshly synthesised nanoparticles, the morphological and elemental analyses were investigated through the JSM-IT800 Schottky Field Emission Scanning Electron Microscope, JEOL Ltd. Investigation involved the utilisation of synthesised materials for the purpose of

conducting an adsorption study. To establish the standard stock solution of chromium (VI) ions with a concentration of 500 parts per million (ppm), a mass of 0.5 gram of chromium was solubilized in 1000 milliliters of distilled water. The initial concentrated solution was subjected to additional dilution in order to attain the desired concentrations, employing the dilution formula denoted as $C_1V_1=C_2V_2$. A solution was prepared and supplemented with 0.1 g of copper oxide nanoparticles (CuO-NPs) and iron(III) oxide (Fe_2O_3) composite. The specimen underwent agitation for approximately 30 minutes within a water bath shaker. Subsequently, the sample was subjected to filtration in order to isolate any remaining Cr (VI) species. The quantification of Cr (VI) was accomplished using Atomic Absorption Spectroscopy (AAS) through the application of **[Eq. 1]**.

$$q_e \left(\frac{mg}{g} \right) \; = \; \frac{C_o - C_e}{W} \times V \qquad \text{[Eq. 1]}$$

Initial and equilibrium concentrations of chromium (VI) metal, denoted as C_o and C_e (mg.L-1) respectively, are of interest in this context. Additionally, the quantity of chromium (VI) adsorbed at equilibrium, represented as q_e (mg/g), and the volume of the solution, denoted as V (mL), are also relevant parameters. The influence of different parameters on the adsorption process was investigated, encompassing temperature, initial concentration, contact time, ionic strength, and pH. The identical methodology was also employed to explore the efficacious elimination of hexavalent chromium (Cr (VI)) from a true sample.

3. Results and Discussion

3.1. Characterization

The synthesis of Fe_2O_3/Cellulose and CuO-NPs was achieved using the co-precipitation method, and the SEM analysis conclusively validates the successful synthesis of these nanomaterials, as showed in [Figure 1]. SEM analysis reveal a densely packed surface with Cr(VI) ions attached to the adsorbent materials. This observation corresponds to the favorable electrostatic interactions and efficient metal adsorption in the acidic environment due to the presence of elevated hydronium ions (H^+). Conversely, under extremely acidic conditions, SEM images show a weakened and less stable adsorbent surface due to surface oxidation processes. This phenomenon aligns with the decrease in metal adsorption observed in these conditions. This shift adversely affects the attachment of chromium oxyanions to the adsorbent surface. The SEM analysis also suggests that at higher pH levels, the presence of an increased concentration of hydroxyl groups (OH^-) in the solution leads to repulsion between chromium oxyanions and OH^- ions, reducing the availability of adsorption sites and competition for these sites.
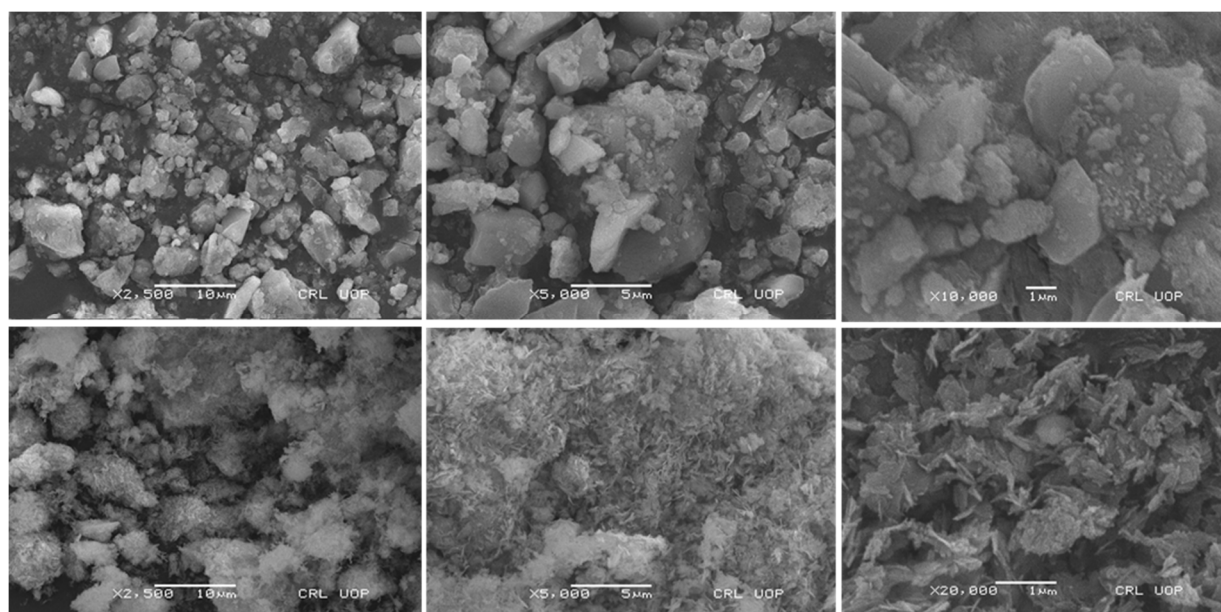
Figure 1. SEM analyses of CuOx nanoparticles (I-III) and FeOx nanoparticles (IV-VII).

3.2. Effect of pH Adsorption and Contact Time

The adsorption behavior of Cr(VI) ions onto the surfaces of Fe_2O_3/cellulose and CuOx nanoparticles (NPs) was investigated across a pH range spanning from 2.0 to 10.0, utilizing a fixed concentration of 300 mg/L. The experimental outcomes are presented graphically in [Figure 2a]. The adsorption of Cr(VI) ions on Fe_2O_3/cellulose and CuOx-NPs displays a significant dependency on pH. Maximum adsorption of Cr(VI) ions was observed at pH values of 2.0 and 4.0. This phenomenon can be attributed to the elevated concentrations of hydronium ions (H+) present on the adsorbent surface within an acidic environment, thereby intensifying the electrostatic interactions between the negatively charged chromium ions and the protonated sorbent.
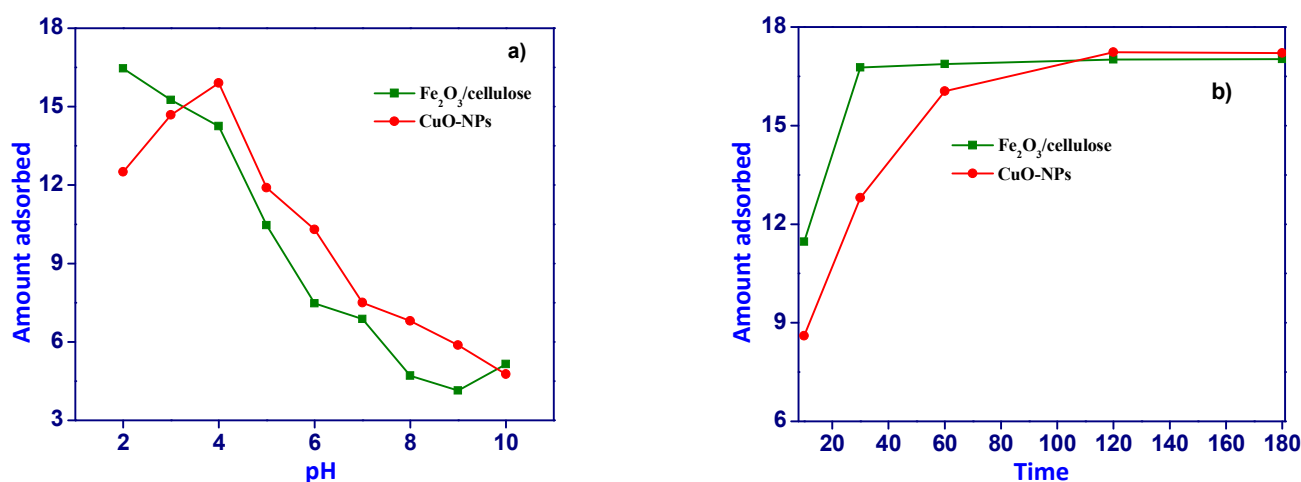
Figure 2. a) Influence of pH on Cr adsorption and b) Impact of Contact Time on Cr adsorption using Fe_2O_3/cellulose and CuO-NPs.

This enhanced interaction enhances the efficiency of metal adsorption. However, it should be noted that the adsorbent surface experiences a weakening and loss of stability under extremely acidic conditions, primarily due to surface oxidation processes, which in turn diminishes the capacity for metal adsorption. These observations are consistent with the fact that CuOx nanoparticles possess a nearly neutral point of zero charge, around 6.9. Consequently, as the pH level rises from its optimal value (pH 3.5) towards the alkaline range, the degree of protonation of the CuOx nanoparticles surface gradually decreases. Beyond this point, the surface acquires a net negative charge, rendering it less favorable for the attachment of chromium oxyanions. Moreover, at higher pH levels, the concentration of hydroxyl groups (OH-) in the solution increases, leading to repulsion between chromium oxyanions and OH- ions, resulting in competition for the limited available adsorption sites. This competition reduces the removal efficiency of Cr(VI) ions from the solution [11-12].

To establish the optimal experimental conditions for the adsorption of Cr(VI) ions onto CuOx nanoparticles (CuOx-NPs) and Fe_2O_3/cellulose composites, we conducted contact time experiments. The findings demonstrated that equilibrium for Cr(VI) ion adsorption on CuOx-NPs was attained after 120 minutes, while equilibrium for adsorption on Fe_2O_3/cellulose was reached within 60 minutes, as illustrated in [Figure 2b]. Initially, the rapid adsorption of Cr(VI) ions was facilitated by the abundance of unoccupied binding sites on the surfaces of CuOx-NPs and Fe_2O_3/cellulose composites, coupled with a substantial concentration gradient between the adsorbate and the solid phase of the synthesized materials. However, with prolonged contact time, the number of available active sites for adsorption diminished, and there was an increase in repulsive forces between the ions that had already adsorbed onto the adsorbent surface and those still in the solution. Consequently,

the adsorption of Cr(VI) ions proceeded more slowly as the system approached equilibrium due to ion competition for the limited accessible binding sites [13-14].

Table 1. Various adsorbent utilized for Cr(VI) adsorption.

S. No	Adsorbent type	Q_{max}(mg/g)	Percent, %	Reference
1	N77 cation exchange resins	35.38mg/g	95	[15]
2	SKN1 cation exchange resins	46.34 mg/g	95	[15]
3	carbon aerogel electrodes	-	94.69	[16]
4	C1 activated carbon	-	98.86	[17]
5	C2 activated carbon	-	98.6	[17]
6	C3 activated carbon		93	[17]
7	Al electrodes	-	97.76	[18]
8	Chemical Precipitation Method		99.74	[18]
9	Eucalyptus bark (EB)	-	99	[19]
10	Cation exchange resins 1200H	84.04 mg/g	-	[20]
11	Cation exchange resins 1500H	188.67 mg/g	-	[20]
12	Cation exchange resins IRN97H	58.14 mg/g	-	[20]
13	Dried green alga U. Lactuca	8.91 mg/g	52.54	[21]
14	Activated carbon	93.92 mg/g	99.52	[21]
15	Activated carbon	28.019 mg/g	-	[22]
16	Electrochemical method	-	86.45	[23]
17	Amidoxime adsorb	31.68 mg/g	-	[24]

3.2. Effect of Adsorbent dosage and Adsorbate Concentration

We conducted an investigation into the effect of adsorbent dosage, with the results presented in [Figure 3a,c]. Upon increasing the adsorbent dose, the removal of Cr(VI) ions exhibited a sharp rise, increasing from 50% to 74.08% for Fe_2O_3/cellulose and from 41% to 78% for CuOx-NPs when initial Cr(VI) ion concentrations were in the range of 1.25 mg/L. Further increases in adsorbent dose led to a gradual enhancement in removal efficiency, reaching 86.97% and 87.44% for Fe_2O_3/cellulose and CuOx-NPs, respectively [Figure 3c]. Conversely, when examining the adsorption capacity of Fe_2O_3/cellulose and CuOx-NPs for an initial Cr(VI) ion concentration of 24 mg/L, it was observed that the adsorption capacity gradually decreased from 80 mg/g to 78 mg/g as the adsorbent dose increased. This phenomenon can be explained by the fact that the ratio of available binding sites to the amount of metal ions in the system affects the adsorbent's capacity for adsorption. At higher doses of Cr(VI) ions, the saturation of binding sites on the surface of CuOx-NPs and Fe_2O_3/cellulose composites was not achieved, resulting in a reduced adsorption capacity per unit mass of CuOx nanoparticles. Furthermore, the increased availability of surface area and open adsorption sites with higher adsorbent dosages contributed to the elevated removal of Cr(VI) ions. However, it should be noted that as equilibrium was approached, additional increases in adsorbent dosage resulted in only marginal improvements in Cr(VI) ion removal. Consequently, a dose of 1.25 g/L was selected for subsequent studies, as it balanced the desirable values of high removal efficiency and adsorption capacity per unit mass of Fe_2O_3/cellulose and CuOx-NPs adsorbent [25-26]. In comparison Table 1., various adsorbent utilized for Cr(VI) adsorption, we examined the impact of varying Cr(VI) ion concentrations on the adsorption behavior of Fe_2O_3/cellulose and CuOx nanoparticles (CuOx-NPs), with the results showed in [Figure 3b]. It was observed that the highest removal efficiencies, reaching 90.04% and 94.08%, were achieved at a relatively low initial metal ion concentration of 5 mg/L. As the initial concentration of Cr(VI) ions was progressively increased from 5 to 50 mg/L, the removal efficiency exhibited a consistent decline, dropping to 69.16% and 62.5%. This phenomenon can be attributed to the availability of a greater number of active surface areas and binding sites on Fe_2O_3/Cellulose and CuOx-NPs when exposed to lower Cr(VI) ion concentrations, resulting in optimal adsorption performance. Conversely, at higher initial concentrations of Cr(VI) ions, fewer

sites were available for the acceptance of Cr(VI) ions on the synthesized materials, thereby leading to a decrease in the adsorption efficiency [27].
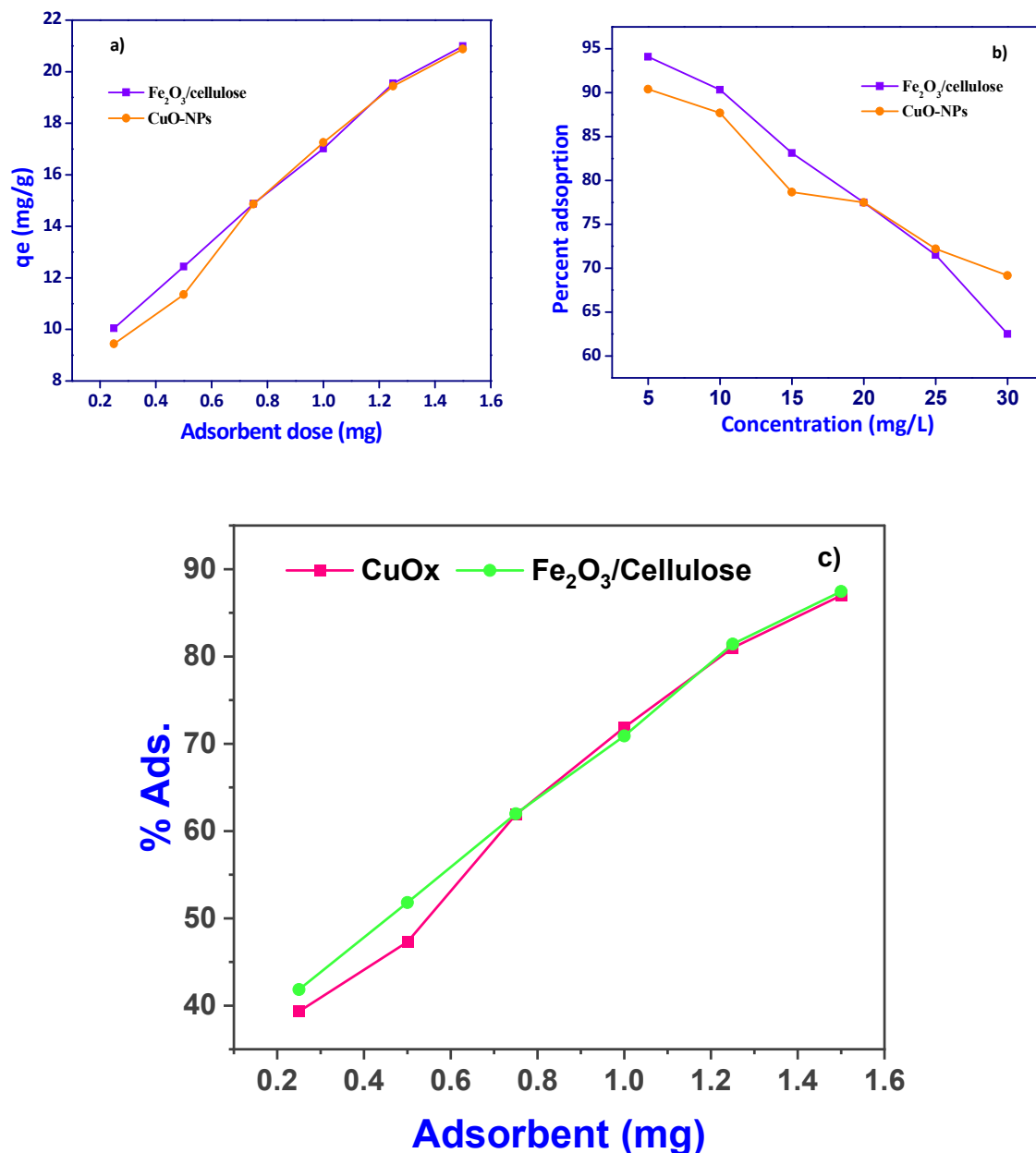

Figure 3. a) Influence of adsorbent on Cr adsorption and b) effect of adsorbate concentration on Cr adsorption using Fe_2O_3/cellulose and CuO-NPs c) .

3.3. Influence of Temperature on Adsorption

A comprehensive investigation into the influence of temperature, spanning from 15°C to 45°C, on the adsorption behavior of Cr(VI) onto the surfaces of Fe_2O_3/Cellulose and CuOx nanoparticles (CuOx-NPs), and the resultant data are visually showed in [Figure 4]. The findings unveiled a distinct temperature-dependent impact on the adsorption process. Specifically, an elevation in temperature within this specified range elicited divergent responses: a notable augmentation in the adsorption of Cr(VI) ions onto CuOx-NPs, in stark contrast to a conspicuous reduction in adsorption observed for Fe_2O_3/cellulose composites. This intriguing phenomenon can be ascribed to the noteworthy reduction

in solution viscosity with increasing temperature, a well-recognized phenomenon in the realm of chemical kinetics. Elevated temperatures serve as a catalyst, enhancing the diffusion rate of adsorbate molecules. This accelerated diffusion occurs both within the exterior boundary layer and, crucially, within the intricate network of pores intrinsic to the adsorbent particles. Consequently, the heightened thermal energy facilitates more efficient interaction between the Cr(VI) ions and the CuOx-NPs, leading to an augmented adsorption capacity. In stark contrast, the adsorption performance of Cr(VI) onto Fe_2O_3/cellulose composites exhibits a counterintuitive decline with rising temperature. This paradoxical behavior can be attributed to complex interplays between temperature-induced changes in the physicochemical properties of the adsorbent and the nature of adsorbate interactions. These interactions influence the availability of active adsorption sites and, consequently, the overall adsorption efficiency [28-29].
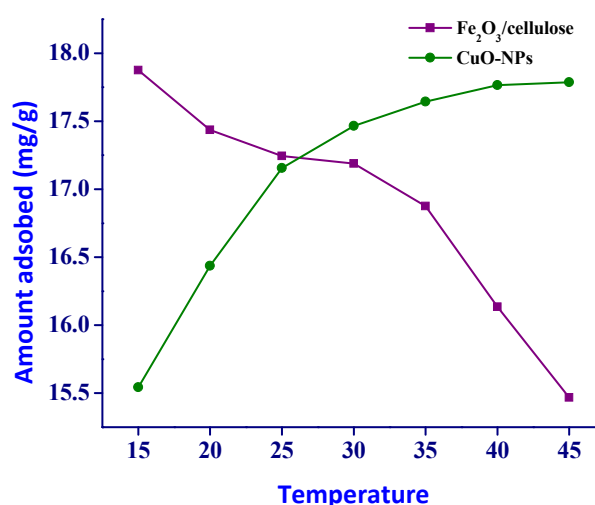
Figure 4. Effect of Temperature on Chromium adsorption utilizing Fe_2O_3/cellulose and CuO-NPs.

3.4. Kinetic Study

Theoretical studies were conducted to study the nature of adsorption and establish potential adsorption mechanisms. To achieve this, well-known adsorption equations and models were utilized to analyze the acquired data. In the kinetic studies, common kinetic models/equations were applied to analyze the adsorption kinetics of the newly developed adsorbent.

3.4.1. Pseudo Second Order Kinetic Model

The model/equation is expressed as:

$$\frac{dq}{dt} = K_2(q_e - q_t)^2$$

The linear form of this model/equation is given as:

$$\frac{t}{q_t} = \frac{t}{q_e} - \frac{1}{K_2 q_e^2}$$

Where qe is the amount of sample adsorbed (mg/g) at equilibrium, qt is the amount of sample adsorbed (mg/g) at any given time (t) (min) and K_2 is the pseudo-second-order reaction rate constant for adsorption (g/mg.min). The constant K_2 = to calculate the initial adsorption rate (h) (mg/g.min), at $t \rightarrow 0$ as follows;

$$h = K_2 q_e^2$$

Where K_2 is the pseudo-second-order reaction rate constant for adsorption (g/mg.min) and qe is the amount of sample adsorbed (mg/g) at equilibrium. From the equilibrium time adsorption data,

the time (t) (min) plotted with t/qt [Figure 5a,b] with correlation co-efficient (R^2) of 0.9958 (slope = 1/qe 0.05418, CuOx), plus R^2 = 0.9958 (1/qe= 0.05762, for Fe_2O_3/cellulose) and the pseudo-second-order-kinetic equation/model were constructed.
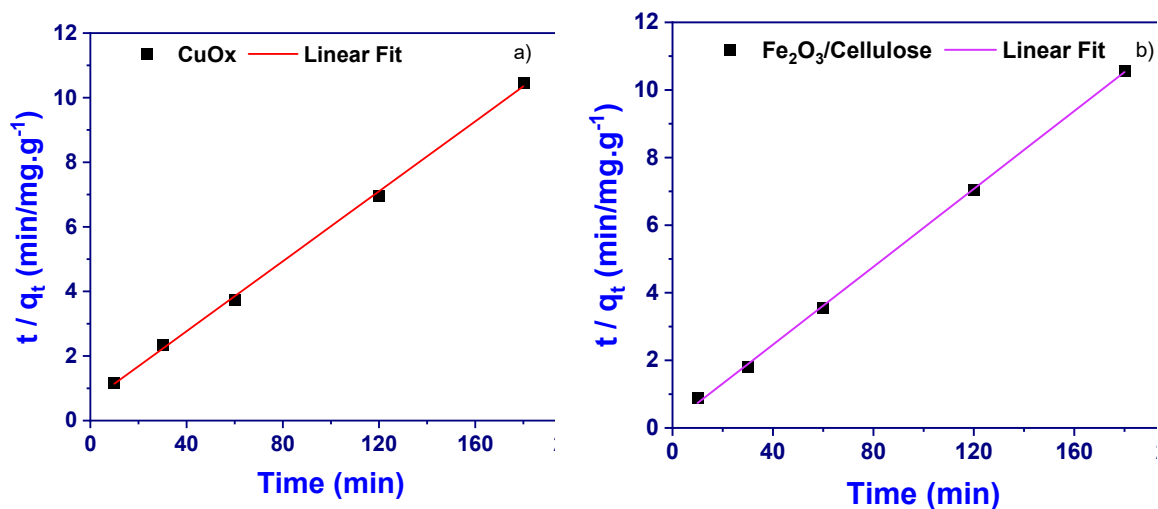
Figure 5. Pseudo second order kinetic model of a) CuOx and b) Fe_2O_3/cellulose.

3.4.2. Langmuir Adsorption Isotherm Model

It is important to establish the most appropriate correlation for the equilibrium curves. An adsorption isotherm/model describes the relationship between the amount of adsorbate that is adsorbed on the adsorbent and the concentration of dissolved adsorbate in the liquid at equilibrium. Isotherm models such as have been used to describe the equilibrium nature of adsorption., the Langmuir adsorption isotherm/model is the most frequently used model for the adsorption of an adsorbate from a liquid solution onto the adsorbent. This model is obtained under the ideal assumption of adsorption surface. It is assumed that adsorbate occupied a site, and no further adsorption occurred a saturated value is reached and no further adsorption can take place. The Langmuir adsorption isotherm/model is used and is expressed by the following equation;

$$q_e = \frac{K_L C_e}{1 + a_L C_e}$$

In a linear form of this equation is given as;

$$\frac{C_e}{q_e} = \frac{1}{K_L} + \frac{a_L C_e}{K_L}$$

Where C_e is the equilibrium concentration of sample (BPB) in the solution (mg/L), q_e is the amount of sample adsorbed (mg/g), K_L and a_L are the Langmuir adsorption isotherm/model constants and are related to the maximum adsorption capacity (L/g) and bonding strength (L/mg), respectively. The theoretical monolayer adsorption capacity (Q_o, mg/g) is numerically equal to K_L/a_L.

$$Q_o = \frac{K_L}{a_L}$$

The C_e (mg/L) was then plotted with C_e/q_e [Figure 6a,b] with correlation co-efficient (R^2) of 0.9907 and the Langmuir adsorption isotherm/model were constructed. In the present study, it is highlighted that the adsorbent is favorable for the adsorption onto the newly developed adsorbent under the studied conditions.
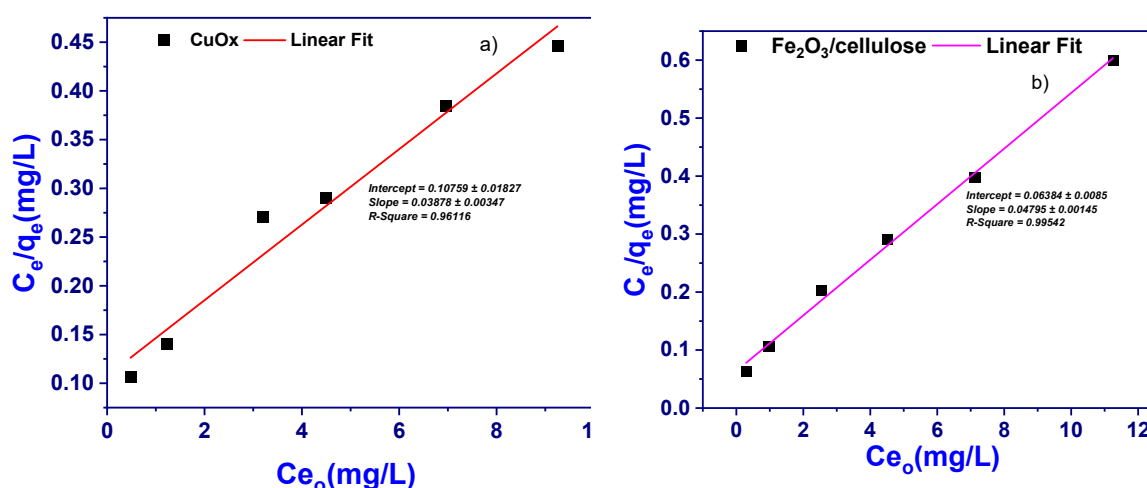
Figure 6. Langmuir adsorption isotherm/model of a) CuOx and b) Fe₂O₃/cellulose.

3.5. Effectiveness of Samples

In the pursuit of evaluating the effectiveness of removing Cr(VI) from authentic and synthetic wastewater samples, we employed Fe_2O_3/cellulose and CuOx nanoparticles (CuOx-NPs) under carefully optimized adsorption parameters, as illustrated in [Figure 7]. This comprehensive assessment encompassed the utilization of three distinct true water samples (comprising tap water, well water, and river water), an industrial effluent sample, and a synthetic wastewater sample. To commence the evaluation process, each of these samples underwent individual spiking with a Cr(VI) concentration of 25 mg/L. Following the completion of the adsorption procedure, we meticulously quantified the amount of adsorbed Cr. The results unveiled a noteworthy accomplishment in the removal of Cr(VI) ions, with removal percentages ranging from 53.52% to 70.97% for authentic water samples and 49.78% to 68.93% for wastewater samples, all facilitated by the utilization of the synthesized composites. These outcomes affirm the practical applicability of the synthesized materials in the purification of authentic water samples, wastewater, and industrial effluents. Remarkably, it is worth noting that Fe_2O_3/cellulose outperformed CuOx-NPs significantly in these diverse applications, underscoring its superior performance [29-30].
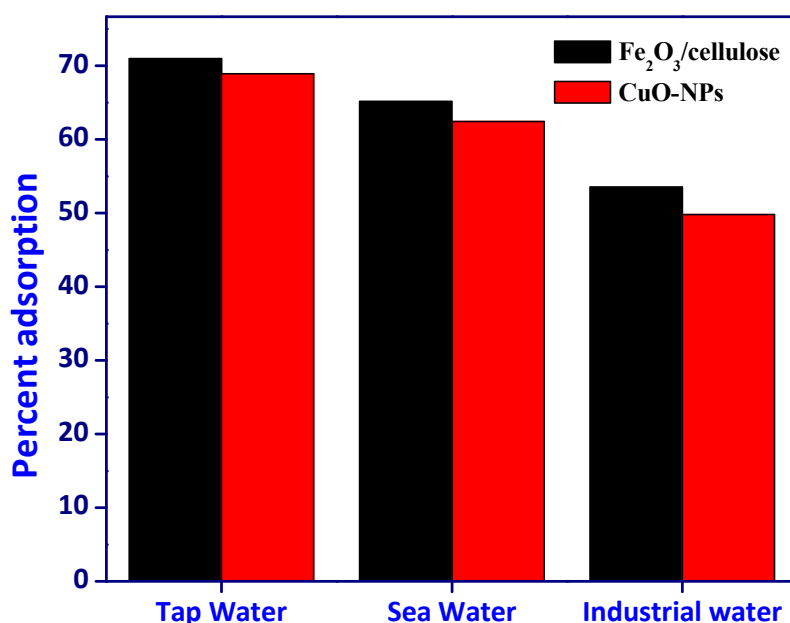
Figure 7. Adsorption of Cr (VI) ion using Fe_2O_3/cellulose and CuO- NPs in true samples.

4. Conclusions

In this study, cellulose-based ferric oxide (Fe_2O_3/cellulose) and copper oxide nanoparticles (CuOx-NPs) were successfully synthesized using the co-precipitation approach. These newly synthesized nanoparticles were extensively characterized the synthesized materials demonstrated promise for the removal of hazardous hexavalent chromium (Cr(VI)) ions from aqueous solutions. The investigation into the effect of pH on Cr(VI) adsorption revealed that the optimal pH for maximum adsorption was 2.0 and 4.0. The impact of adsorbent dosage indicated that an increase in dosage led to enhanced Cr(VI) ion removal, with saturation observed at higher doses. Furthermore, the influence of adsorbate concentration on adsorption performance demonstrated that lower initial Cr(VI) ion concentrations resulted in higher removal efficiencies. Thermal influence on adsorption investigated, with CuOx-NPs exhibiting increased adsorption at higher temperatures, attributed to enhanced diffusion rates. Conversely, Fe_2O_3/cellulose composites showed decreased adsorption at elevated temperatures, likely due to altered surface properties. The practical applicability of Fe_2O_3/cellulose and CuOx-NPs were confirmed through successful Cr(VI) ion removal from real water samples, including tap water, well water, river water, and industrial effluent. These findings highlight the potential of these nanomaterials for efficient and sustainable heavy metal ion removal from aqueous environments, addressing environmental contamination concerns.

Conflicts of Interest: The authors declare no conflicts of interest.

References

1. Gautam, R. K., Sharma, S. K., Mahiya, S., & Chattopadhyaya, M. C. (2014). Contamination of heavy metals in aquatic media: transport, toxicity and technologies for remediation.

2. Gupta, A., Singh, A., & Mishra, V. K. (2023). Hexavalent Cr, Its Toxicity and Removal Strategy: Revealing PGPB Potential in Its Remediation. Water, Air, & Soil Pollution, 234(8), 492.

3. Ma, T., Ding, Y., Xu, F., Zhang, C., Zhou, M., Tang, Y., ... & Wang, S. Effects of Acute and Chronic Heavy Metal Chromium Stress on Heat Shock Protein Gene and Antioxidant Enzyme Activities of Orthetrum Albistylum Larvae. Available at SSRN 4508988.

4. Kurniawan, T. A., Othman, M. H. D., Adam, M. R., Liang, X., Goh, H., Anouzla, A., ... & Chew, K. W. (2023). Chromium Removal from Aqueous Solution Using Natural Clinoptilolite. Water, 15(9), 1667.

5. Ding, Z. J., Liu, Y., Weerasooriya, R., & Chen, X. (2023). Electrochemical Determination of Chromium (VI) with Au/UiO-66 Modified Glassy Carbon and Screen-Printed Electrodes by Linear Sweep Voltammetry (LSV). Analytical Letters, 1-19.

6. Shrestha, R., Ban, S., Devkota, S., Sharma, S., Joshi, R., Tiwari, A. P., ... & Joshi, M. K. (2021). Technological trends in heavy metals removal from industrial wastewater: A review. Journal of Environmental Chemical Engineering, 9(4), 105688.

7. Barakat, M. A. (2011). New trends in removing heavy metals from industrial wastewater. Arabian journal of chemistry, 4(4), 361-377.

8. Shaabani, A., Nosrati, H., & Seyyedhamzeh, M. (2015). Cellulose@ Fe 2 O 3 nanoparticle composites: magnetically recyclable nanocatalyst for the synthesis of 3-aminoimidazo [1, 2-a] pyridines. Research on Chemical Intermediates, 41, 3719-3727.

9. Luna, I. Z., & Bangladesh Atomic Energy Commission. (2015). Preparation and characterization of copper oxide nanoparticles synthesized via chemical precipitation method. Open Access Library Journal, 2(03), 1.

10. Nogueira, A. E., Giroto, A. S., Neto, A. B., & Ribeiro, C. (2016). CuO synthesized by solvothermal method as a high capacity adsorbent for hexavalent chromium. Colloids and Surfaces A: Physicochemical and Engineering Aspects, 498, 161-167.

11. A.U. Haq, M. Saeed, M. Usman, M. Yameen, M. Muneer, S. Tubbsum, A comparative sorption study of Cr3+ and Cr6+ using mango peels: kinetic, equilibrium and thermodynamic, Green Processing and Synthesis, 8, 337-347(2019).

12. X.H. Vu, L.H. Nguyen, H.T. Van, D.V. Nguyen, T.H. Nguyen, Q.T. Nguyen, L. Ha, Adsorption of chromium(VI) onto freshwater snail shell-derived biosorbent from aqueous solutions: Equilibrium, kinetics, and thermodynamics, Journal of Chemistry, Article ID: 3038103, 1-11(2019).

13. S. Tamjidi, H. Esmaeili, Chemically modified CaO/Fe3O4 nanocomposite by sodium dodecyl sulfate for Cr(III) removal from water, Chemical Engineering and Technology, 42, 607-616(2019).

14. J. Wang, R. Cao, D. He, A. Saleem, Facile preparation of polyethyleneimine modified activated sludge-based adsorbent for hexavalent chromium removal from aqueous solution, Separation Science and Technology,56,498-506 (2021).

15. Rengaraj, S., Yeon, K. H., & Moon, S. H. (2001). Removal of chromium from water and wastewater by ion exchange resins. Journal of hazardous materials, 87(1-3), 273-287.

16. Rana, P., N. Mohan, and C. Rajagopal. "Electrochemical removal of chromium from wastewater by using carbon aerogel electrodes." Water research 38.12 (2004): 2811-2820.

17. Fahim, N. F., et al. "Removal of chromium (III) from tannery wastewater using activated carbon from sugar industrial waste." Journal of Hazardous Materials 136.2 (2006): 303-309.

18. Mella, B., Glanert, A. C., & Gutterres, M. (2015). Removal of chromium from tanning wastewater and its reuse. Process Safety and Environmental Protection, 95, 195-201.

19. Sarin, Vikrant, and K_K Pant. "Removal of chromium from industrial waste by using eucalyptus bark." Bioresource technology 97.1 (2006): 15-20.

20. Rengaraj, S., et al. "Kinetics of removal of chromium from water and electronic process wastewater by ion exchange resins: 1200H, 1500H and IRN97H." Journal of hazardous materials 102.2-3 (2003): 257-275.

21. El-Sikaily, Amany, et al. "Removal of toxic chromium from wastewater using green alga Ulva lactuca and its activated carbon." Journal of hazardous materials 148.1-2 (2007): 216-228.

22. Acharya, Jyotikusum, et al. "Removal of chromium (VI) from wastewater by activated carbon developed from Tamarind wood activated with zinc chloride." Chemical Engineering Journal 150.1 (2009): 25-39.

23. Peng, Hao, Yumeng Leng, and Jing Guo. "Electrochemical removal of chromium (VI) from wastewater." Applied sciences 9.6 (2019): 1156.

24. Hayashi, Natsuki, Jinhua Chen, and Noriaki Seko. "Nitrogen-containing fabric adsorbents prepared by radiation grafting for removal of chromium from wastewater." Polymers 10.7 (2018): 744.

25. N.H. Kera, M. Bhaumik, K. Pillay, S.S. Ray, A. Maity, Selective removal of toxic Cr(VI) from aqueous solution by adsorption combined with reduction at a magnetic nanocomposite surface, Journal of Colloid and Interface Science, 503,214-228(2017).

26. Y. Chen, H. Xu, S. Wang, L. Kang, Removal of Cr(VI) from water using polypyrrole/attapulgite core-shell nanocomposites: equilibrium, thermodynamics and kinetics, RSC Advances, 4,17805-17811(2014).

27. M.A. Atieh, O.Y. Bakather, B.S. Tawabini, A.A. Bukhari, M. Khaled, M. Alharthi, M. Fettouhi, F.A.Abuilaiwi, Removal of chromium(III) from water by using modified and nonmodified carbon nanotubes, Journal of Nanomaterials, 2010, 34-39 (2010).
28. F. Ahmadi, H. Esmaeili, Chemically modified bentonite/Fe3O4 nanocomposite for Pb(II), Cd(II), and Ni(II) removal from synthetic wastewater, Desalination and Water Treatment,110, 154-167(2018).
29. S. Egodawatte, A. Datt, E.A. Burns, S.C. Larsen, Chemical insight into the adsorption of chromium(III) on iron oxide/mesoporous silica nanocomposites, Langmuir, 31,7553-7562(2015).
30. L.P. Lingamdinne, I.-S. Kim, J.-H. Ha, Y.-Y. Chang, J.R. Koduru, J.-K. Yang, Enhanced adsorption removal of Pb(II) and Cr(III) by using nickel ferrite-reduced graphene oxide nanocomposite, Metals, 7, 225-234 (2017).